

Constraints on the momentum dependence of nuclear symmetry potential from Sn + Sn collisions at 270 MeV/nucleon

Gao-Feng Wei,^{1,2,*} Xin Huang,¹ Qi-Jun Zhi,^{1,2} Ai-Jun Dong,^{1,2} Chang-Gen Peng,³ and Zheng-Wen Long⁴

¹*School of Physics and Electronic Science, Guizhou Normal University, Guiyang 550025, China*

²*Guizhou Provincial Key Laboratory of Radio Astronomy and Data Processing,
Guizhou Normal University, Guiyang 550025, China*

³*Guizhou Provincial Key Laboratory of Public Big Data, Guizhou University, Guiyang 550025, China*

⁴*College of Physics, Guizhou University, Guiyang 550025, China*

Within a transport model, we employ the central Sn + Sn collisions at 270 MeV/nucleon to constrain the momentum dependence of nuclear symmetry potential that can be characterised by the value of nuclear symmetry potential at the saturation density and infinitely large nucleon momentum, i.e., $U_{sym}^{\infty}(\rho_0)$. Through comparing the charged pion yields as well as their single and double pion ratios of the theoretical simulations for the reactions $^{108}\text{Sn} + ^{112}\text{Sn}$ and $^{132}\text{Sn} + ^{124}\text{Sn}$ with the corresponding data in S π RIT experiments, as well as conducting the corresponding χ -square analyses, the value of $U_{sym}^{\infty}(\rho_0)$ is constrained between -171.5 and -138.6 MeV that ensures the errors between theoretical simulations of pion observables and corresponding data in S π RIT experiments to be within 4%. Moreover, the related isospin splitting of in-medium nucleon effective mass is also discussed within the constrained $U_{sym}^{\infty}(\rho_0)$.

I. INTRODUCTION

The equation of state (EoS) of asymmetric nuclear matter (ANM) especially its nuclear symmetry energy term plays an essential role in studying the structure and evolution of radioactive nuclei as well as the synthesis of medium and heavy nuclei [1–9]. The nuclear symmetry energy characterizes the variation of EoS of the symmetric nuclear matter (SNM) to that of the pure neutron matter (PNM), the latter is closely connected to the neutron star (NS) matter. Naturally, the properties of NS such as the radius as well as the deformation of NS merger are also closely related to the nuclear symmetry energy especially that at densities of about twice the saturation density ρ_0 [10–17]. Nevertheless, knowledge on the nuclear symmetry energy at suprasaturation densities is still far from satisfactory so far, although that around and below ρ_0 [18] as well as the isospin-independent part of EoS for ANM, i.e., EoS of SNM [19, 20], are relatively well determined. Essentially, the EoS of ANM and its nuclear symmetry energy term are determined by the nuclear mean field especially its isovector part, i.e., the nuclear symmetry potential. However, because of the extreme challenge of relatively direct detection of nuclear symmetry potential in experiments, one only extracted using the nucleon-nucleus scattering and (p,n) charge-exchange reactions between isobaric analog states limited information of nuclear symmetry potential at ρ_0 , and parameterized as $U_{sym}(\rho_0, E_k) = a - bE_k$, where $a \approx 22 - 34$ MeV, $b \approx 0.1 - 0.2$ and E_k is limited to no more than 200 MeV [21–23].

Heavy-ion collision (HIC) using some isospin-sensitive observables is one of the most promising approaches to explore the nuclear symmetry potential/energy especially

at suprasaturation densities [3, 4, 10, 24–26]. Very recently, the S π RIT collaboration reported the results from the first measurement dedicated to probe the nuclear symmetry energy at suprasaturation densities via pion production in Sn + Sn collisions at 270 MeV/nucleon carried out at RIKEN-RIBF in Japan [24]. Moreover, they compared the charged pion yields as well as their single and double pion ratios with the corresponding simulation results from seven transport models. Qualitatively, the theoretical simulations from seven transport models reach an agreement with the data, yet quantitatively, almost all the models cannot very satisfactorily reproduce both the pion yields and their single as well as double pion ratios of the experimental data [24]. To this situation, author in Ref. [27] claimed that through considering about 20% high momentum nucleons with momentum up to 1.75 times of Fermi momentum in colliding nuclei can reproduce quite well both the charged pion yields and their single as well as double pion ratios of the experimental data, due to the fact that high momentum distribution in nuclei caused by the short-range correlations (SRCs) has been strongly demonstrated both in experiments and theories [28–33]. Actually, apart from the high momentum nucleon distribution, the momentum dependence of nuclear symmetry potential plays a more important role in probing the high density nuclear symmetry energy [34–36]. As indicated in Ref. [24], the possible reasons for the unsatisfactory of seven models quantitatively fitting experimental data may be different assumptions regarding the mean field potential, pion potential as well as the treatment of Coulomb field. Therefore, it is very necessary to explore how these factors affect the pion production in HICs. More importantly, whether can one make some constraints on these uncertain factors using these high precision pion data of S π RIT experiments [24].

In this paper, after incorporating the SRCs effects into the colliding nuclei similar as that in Ref. [27], we focus

* E-mail: wei.gaofeng@gznu.edu.cn

on the momentum dependence of nuclear symmetry potential that has been shown to be very important for pion production in HICs [37, 38] but has not been well constrained so far. As to other factors indicated in Ref. [24], we also give detailed consideration according to some sophisticated treatment ways as discussed in Sec. II. In Sec. III, we discuss the results of the present study. A summary is given finally in Sec. IV.

II. THE MODEL

This study is carried out within an isospin- and momentum-dependent Boltzmann-Uehling-Uhlenbeck (IBUU) transport model. In the framework, the present version of IBUU model originates from the IBUU04 [37, 38] and/or IBUU11 [39] models. However, the present version of IBUU model has been greatly improved to achieve more accurate simulations of the pion production as discussed in the following.

First, a separate density-dependent scenario for the in-medium nucleon-nucleon interaction [40–42], i.e.,

$$v_D = t_0(1 + x_0 P_\sigma)[\rho_{\tau_i}(\mathbf{r}_i) + \rho_{\tau_j}(\mathbf{r}_j)]^\alpha \delta(\mathbf{r}_{ij}), \quad (1)$$

is used to replace the density-dependent term of original Gogny effective interaction [43], i.e.,

$$v(r) = \sum_{i=1,2} (W + BP_\sigma - HP_\tau - MP_\sigma P_\tau)_i e^{-r^2/\mu_i^2} + t_0(1 + x_0 P_\sigma) \left[\rho \left(\frac{\mathbf{r}_i + \mathbf{r}_j}{2} \right) \right]^\alpha \delta(\mathbf{r}_{ij}), \quad (2)$$

where W , B , H , M , and μ are five parameters, P_τ and P_σ are the isospin and spin exchange operators, respectively; while α is the density dependent parameter used to mimic in-medium effects of the many-body interactions [40–42]. Correspondingly, the potential energy density for ANM with this improved momentum-dependent interaction (IMDI) is expressed [41] as

$$V(\rho, \delta) = \frac{A_u(x)\rho_n\rho_p}{\rho_0} + \frac{A_l(x)}{2\rho_0}(\rho_n^2 + \rho_p^2) + \frac{B}{\sigma+1} \frac{\rho^{\sigma+1}}{\rho_0^\sigma} \times \left\{ \frac{1+x}{2}(1-\delta)^2 + \frac{1-x}{4}[(1+\delta)^{\sigma+1} + (1-\delta)^{\sigma+1}] \right\} + \frac{1}{\rho_0} \sum_{\tau, \tau'} C_{\tau, \tau'} \int \int d^3p d^3p' \frac{f_\tau(\vec{r}, \vec{p}) f_{\tau'}(\vec{r}, \vec{p}')}{1 + (\vec{p} - \vec{p}')^2/\Lambda^2}. \quad (3)$$

In the mean-field approximation, Eq. (3) leads to the following single-nucleon potential for the present IBUU model [40–42],

$$U(\rho, \delta, \vec{p}, \tau) = A_u(x) \frac{\rho_{-\tau}}{\rho_0} + A_l(x) \frac{\rho_\tau}{\rho_0} + \frac{B}{2} \left(\frac{2\rho_\tau}{\rho_0} \right)^\sigma (1-x) + \frac{2B}{\sigma+1} \left(\frac{\rho}{\rho_0} \right)^\sigma (1+x) \frac{\rho_{-\tau}}{\rho} \left[1 + (\sigma-1) \frac{\rho_\tau}{\rho} \right] + \frac{2C_l}{\rho_0} \int d^3p' \frac{f_\tau(\vec{p}')}{1 + (\vec{p} - \vec{p}')^2/\Lambda^2} + \frac{2C_u}{\rho_0} \int d^3p' \frac{f_{-\tau}(\vec{p}')}{1 + (\vec{p} - \vec{p}')^2/\Lambda^2}, \quad (4)$$

where $\sigma = \alpha + 1$, $\tau = 1$ for neutrons and -1 for protons, and the parameters $A_u(x)$, $A_l(x)$, C_u ($\equiv C_{\tau, -\tau}$) and C_l ($\equiv C_{\tau, \tau}$) are expressed as

$$A_l(x) = A_{l0} + U_{sym}^\infty(\rho_0) - \frac{2B}{\sigma+1} \times \left[\frac{(1-x)}{4} \sigma(\sigma+1) - \frac{1+x}{2} \right], \quad (5)$$

$$A_u(x) = A_{u0} - U_{sym}^\infty(\rho_0) + \frac{2B}{\sigma+1} \times \left[\frac{(1-x)}{4} \sigma(\sigma+1) - \frac{1+x}{2} \right], \quad (6)$$

$$C_l = C_{l0} - 2U_{sym}^\infty(\rho_0) \frac{p_{f0}^2}{\Lambda^2 \ln [(4p_{f0}^2 + \Lambda^2)/\Lambda^2]}, \quad (7)$$

$$C_u = C_{u0} + 2U_{sym}^\infty(\rho_0) \frac{p_{f0}^2}{\Lambda^2 \ln [(4p_{f0}^2 + \Lambda^2)/\Lambda^2]}, \quad (8)$$

where p_{f0} is the nucleon Fermi momentum in SNM at ρ_0 , and $U_{sym}^\infty(\rho_0)$ is used to characterize the momentum dependence of nuclear symmetry potential at ρ_0 . Presently, knowledge on the momentum dependence of nuclear symmetry potential even at ρ_0 is rather limited as aforementioned [21–23]. Therefore, taking the current consensus on the momentum dependence of nuclear symmetry potential as a reference, we treat the $U_{sym}^\infty(\rho_0)$ as a free parameter similar as the x parameter, that is used to mimic the slope value $L \equiv 3\rho(dE_{sym}/d\rho)$ of nuclear symmetry energy at ρ_0 without changing the value of nuclear symmetry energy $E_{sym}(\rho)$ at ρ_0 and any properties of the SNM. Actually, a similar quantity (i.e., y parameter) in Refs. [44, 45] has been used to describe the momentum dependence of nuclear symmetry potential at ρ_0 , however, the quantitative constraints on it are not concluded. In addition, it should be mentioned that the B -terms in Eqs. (3) and (4) as well as in the expressions of A_u and A_l are completely different from that in Refs. [44, 45]. This is exactly because the separate density-dependent scenario for in-medium nucleon-nucleon interaction has been adopted in the present model to more delicate treatment of the in-medium many-body force effects [41] that also affects significantly the pion production in HICs [42]. The parameters A_{l0} , A_{u0} , B , σ , C_{l0} , C_{u0} and Λ are determined as that in Ref. [44] by experimental and/or empirical constraints on properties of nuclear matter at $\rho_0 = 0.16 \text{ fm}^{-3}$, i.e., the binding energy -16 MeV , the incompressibility $K_0 = 230 \text{ MeV}$ for SNM, the isoscalar effective mass $m_s^* = 0.7m$, the isoscalar potential at infinitely large nucleon momentum $U_0^\infty(\rho_0) = 75 \text{ MeV}$, as well as the nuclear symmetry energy $E_{sym}(\rho_0) = 32.5 \text{ MeV}$. The values of these parameters are $A_{l0} = A_{u0} = -66.963 \text{ MeV}$, $B = 141.963 \text{ MeV}$, $C_{l0} = -60.486 \text{ MeV}$, $C_{u0} = -99.702 \text{ MeV}$, $\sigma = 1.2652$, and $\Lambda = 2.424p_{f0}$.

Shown in Fig. 1 is the kinetic-energy dependent isoscalar potential at ρ_0 calculated from the IMDI interaction in comparison with the Schrödinger-equivalent isoscalar potential obtained by Hama *et al.* [46, 47]. Obvi-

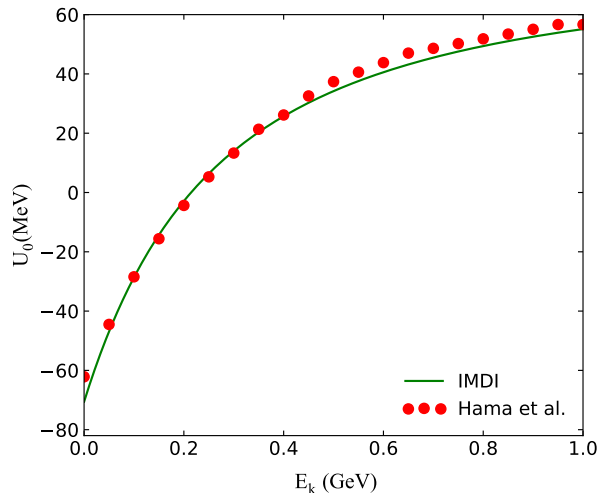


FIG. 1. (Color online) Kinetic-energy dependent isoscalar potentials at ρ_0 calculated from the IMDI interaction in comparison with the Schrödinger-equivalent isoscalar potential obtained by Hama *et al.*

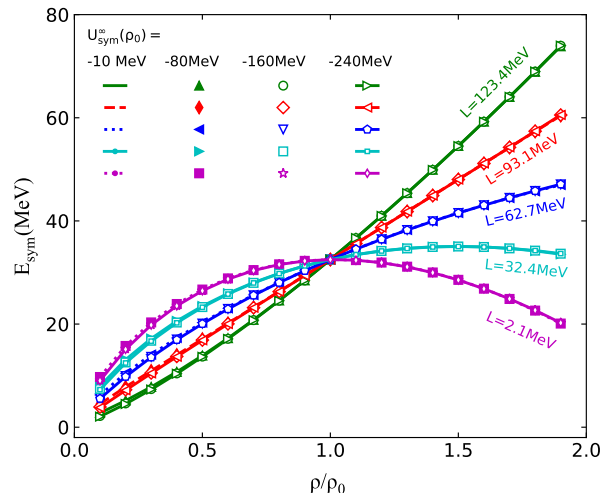


FIG. 3. (Color online) Density dependence of the nuclear symmetry energy with different $U_{sym}^{\infty}(\rho_0)$ calculated from the IMDI interaction.

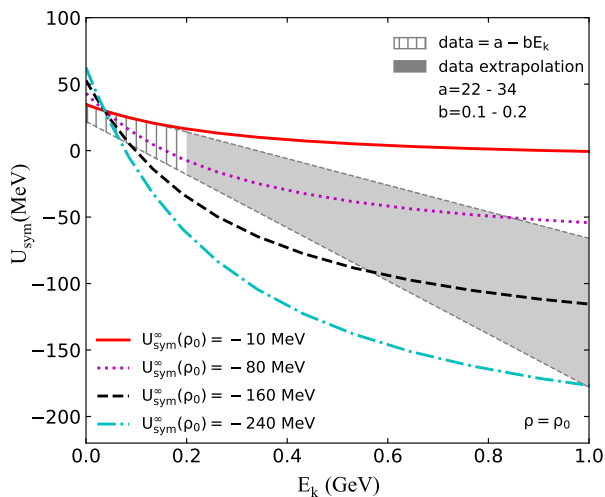


FIG. 2. (Color online) Momentum/kinetic-energy dependent nuclear symmetry potential at ρ_0 with different $U_{sym}^{\infty}(\rho_0)$ calculated from the IMDI interaction and that from the experimental and/or empirical data.

ously, quite good consistency can be seen for the isoscalar potential between the present model and that of the Hama *et al.* Shown in Fig. 2 are the momentum/kinetic-energy dependent nuclear symmetry potential at ρ_0 with different $U_{sym}^{\infty}(\rho_0)$ calculated from the IMDI interaction and the parameterized one from the experimental and/or empirical data [21–23]. To provide more intuitive references for the $U_{sym}^{\infty}(\rho_0)$, we also extrapolate the experimental and/or empirical nuclear symmetry potential to nucleon kinetic energy up to 1 GeV. It is seen that the larger value for the $|U_{sym}^{\infty}(\rho_0)|$ leads to the greater strength and steeper slope for the nuclear symmetry po-

tential at ρ_0 (and also other densities). Moreover, the value of our nuclear symmetry potentials at Fermi kinetic energy (i.e., about 36.8 MeV) even with different $U_{sym}^{\infty}(\rho_0)$ is the same and also within the allowed range of experimental and/or empirical data. At the zero kinetic energy, the value of nuclear symmetry potentials with some settings for the $U_{sym}^{\infty}(\rho_0)$ is slightly higher than that of experimental and/or empirical data. However, this is expected to less affect the pion production since the pion is produced mainly from the energetic nucleon-nucleon inelastic collisions in HICs. On the other hand, since the isoscalar potentials are unchanged with different $U_{sym}^{\infty}(\rho_0)$, one naturally expects the differences of momentum dependence between nuclear symmetry potentials with different $U_{sym}^{\infty}(\rho_0)$ can be reflected by the pion observable in HICs, because the stronger nuclear symmetry potential can lead to the larger isospin effects, i.e., the larger π^-/π^+ ratios for neutron-rich reactions. Nevertheless, to get the pion observable more cleanly reflecting effects of the momentum dependence of nuclear symmetry potential, the effects of high density symmetry energy (i.e., L that is controlled by the x parameter) on the pion observable should be isolated. To this end, it is useful to map the momentum dependent nuclear symmetry potential with different $U_{sym}^{\infty}(\rho_0)$ into the same nuclear symmetry energy. This is carried out by fitting the identical constraints for SNM as well as the identical slope parameter of nuclear symmetry energy at ρ_0 , the corresponding results are also shown in Fig. 3. It is seen that even with the same nuclear symmetry energy, the corresponding nuclear symmetry potential could be very different. Actually, according to the relation between the nuclear symmetry energy and the single-nucleon potential [34–36], i.e., $E_{sym}(\rho) \approx \frac{1}{3}t(k_F) + \frac{1}{6}\frac{\partial U_0}{\partial k}|_{k_F} k_F + \frac{1}{2}U_{sym}(k_F)$, the contribution of nuclear symmetry potential to the nuclear symmetry energy depends only on its value at

Fermi momentum/kinetic-energy.

Second, to more accurate simulations of pion production in HICs, we also consider the Δ potential and pion potential effects in HICs. For the Δ potential, instead of using the usual ansatz of setting the Δ potential equal to that of nucleons that might lead to incorrect π^- and π^+ production thresholds and total multiplicities as indicated in Refs. [10, 24], we adjust the depth of Δ potential by a factor $2/3$ to that of nucleons due to the fact that the depth of nucleon potential is approximately -50 MeV while that of the Δ potential is empirically constrained around -30 MeV [47–50], for the specific expression of the Δ potential, see Ref. [51] for the details. Pion potential is another factor that also might affect the pion production in HICs as indicated in Refs. [10, 24, 52–55]. Therefore, we also consider the pion potential effects in this study. Specifically, when the pionic momentum is higher than 140 MeV/ c , we use the pion potential based on the Δ -hole model, of the form adopted in Ref. [47]; when the pionic momentum is lower than 80 MeV/ c , we adopt the pion potential of the form used in Refs. [48–50]; while for the pionic momentum falling into the range from 80 to 140 MeV/ c , an interpolative pion potential constructed in Ref. [47] is used. It should be mentioned that the present pion potential includes the isospin- and momentum-dependent pion s -wave and p -wave potentials in nuclear medium as that in Ref. [55], see Refs. [47–50] for the details.

Finally, as to the treatment of Coulomb field as indicated in Refs. [10, 24], we calculate self-consistently the electromagnetic (EM) interactions from the Maxwell equation, i.e., $\mathbf{E} = -\nabla\varphi - \partial\mathbf{A}/\partial t$, $\mathbf{B} = \nabla \times \mathbf{A}$, where the scalar potential φ and vector potential \mathbf{A} of EM fields are also calculated self-consistently from the resources of charges Ze and currents $Ze\mathbf{v}$. Actually, the necessity of self-consistent calculations regarding the EM fields in HICs has been verified in reactions $^{96}\text{Ru} + ^{96}\text{Ru}$ and $^{96}\text{Zr} + ^{96}\text{Zr}$ at 400 MeV/nucleon [51]. Certainly, for the studied reactions Sn + Sn at 270 MeV/nucleon, the simplified Liénard-Wiechert formulas by neglecting the radiation fields for calculations of EM fields in HICs might be enough. For the detailed EM field effects in HICs, we refer readers to Refs. [51, 56, 57] for more details.

III. RESULTS AND DISCUSSIONS

Now, we turn to the pion production in $^{108}\text{Sn} + ^{112}\text{Sn}$ and $^{132}\text{Sn} + ^{124}\text{Sn}$ reactions at 270 MeV/nucleon with an impact parameter of $b = 3$ fm. To study the sensitivities of pion yields on the high density symmetry energy (i.e., L) and the momentum dependence of nuclear symmetry potential (i.e., $U_{sym}^\infty(\rho_0)$), pion yields as a function of the L for different $U_{sym}^\infty(\rho_0)$ settings in the reactions are shown in Fig. 4. First, consistent with the findings in Refs. [27, 58], it is seen that the multiplicities of π^- are more sensitive to the L compared to those of π^+ , in particular for the larger isospin asymmetry reactions

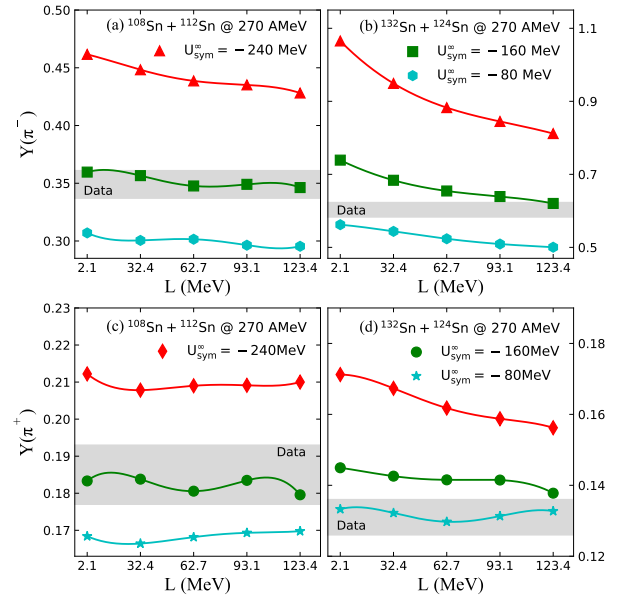


FIG. 4. (Color online) Upper: Multiplicities of π^- generated in reactions $^{108}\text{Sn} + ^{112}\text{Sn}$ (a) and $^{132}\text{Sn} + ^{124}\text{Sn}$ (b) with different $U_{sym}^\infty(\rho_0)$ as a function of the L in comparison with the corresponding S π RIT data; Lower: Multiplicities of π^+ generated in reactions $^{108}\text{Sn} + ^{112}\text{Sn}$ (c) and $^{132}\text{Sn} + ^{124}\text{Sn}$ (d) with different $U_{sym}^\infty(\rho_0)$ as a function of the L in comparison with the corresponding S π RIT data.

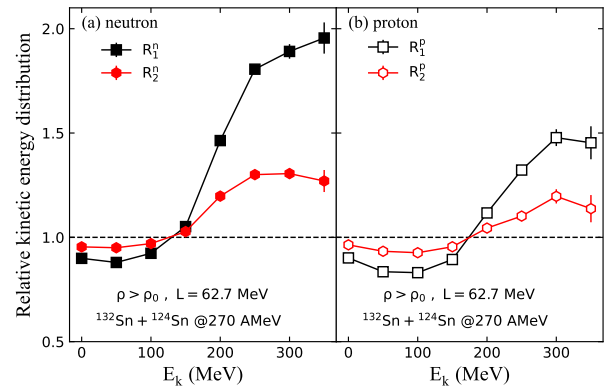


FIG. 5. (Color online) Relative kinetic energy distribution of nucleons with local densities higher than ρ_0 at the maximum compress stage in central $^{132}\text{Sn} + ^{124}\text{Sn}$ reactions at 270 MeV/nucleon.

$^{132}\text{Sn} + ^{124}\text{Sn}$, since the π^- is mostly produced from the neutron-neutron inelastic collisions [58]. Second, it is seen that with a certain L value the stronger nuclear symmetry potential with larger value of $|U_{sym}^\infty(\rho_0)|$ leads to more production of π^- and π^+ . To understand this observation, we can check the kinetic energy distribution of nucleons with local densities higher than ρ_0 at the compress stage in the reactions, due to the π^- and π^+ are produced mainly from energetic nn and pp inelastic colli-

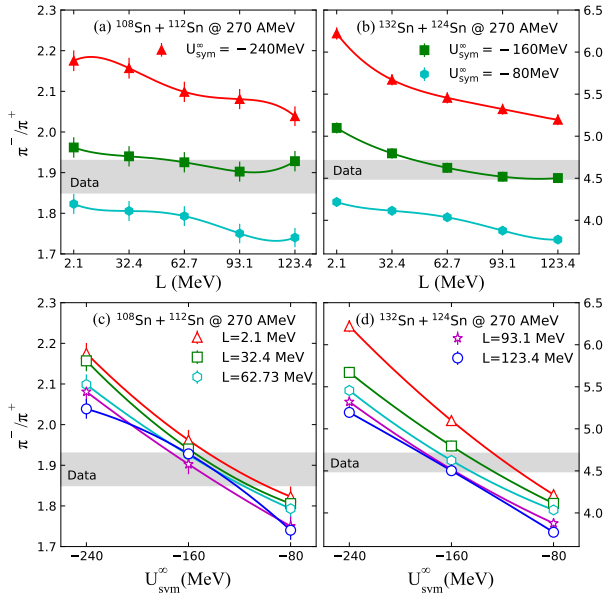


FIG. 6. (Color online) Upper: Ratios of π^-/π^+ generated in reactions $^{108}\text{Sn} + ^{112}\text{Sn}$ (a) and $^{132}\text{Sn} + ^{124}\text{Sn}$ (b) with different $U_{sym}^\infty(\rho_0)$ as a function of the L in comparison with the corresponding S π RIT data; Lower: Ratios of π^-/π^+ generated in reactions $^{108}\text{Sn} + ^{112}\text{Sn}$ (c) and $^{132}\text{Sn} + ^{124}\text{Sn}$ (d) with different L as a function of the $U_{sym}^\infty(\rho_0)$ in comparison with the corresponding S π RIT data.

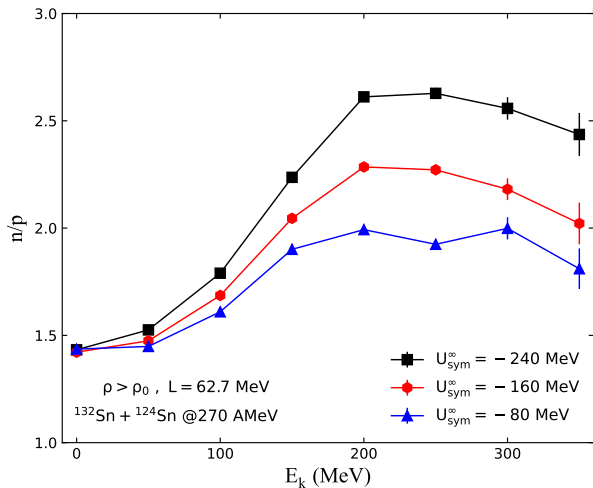


FIG. 7. (Color online) Kinetic energy distribution of neutrons over protons n/p with local densities higher than ρ_0 produced at the maximum compress stage in the reaction $^{132}\text{Sn} + ^{124}\text{Sn}$ with different $U_{sym}^\infty(\rho_0)$ and a certain L .

sions at the compress stage, respectively. To this end, we examine the relative kinetic energy distribution of nucleons with local densities higher than ρ_0 at the maximum

compress stage through the following ratios:

$$R_1^i = \frac{\text{number}(i)_{U_{sym}^\infty = -240}}{\text{number}(i)_{U_{sym}^\infty = -80}}, \quad (9)$$

$$R_2^i = \frac{\text{number}(i)_{U_{sym}^\infty = -160}}{\text{number}(i)_{U_{sym}^\infty = -80}}, \quad (10)$$

where i denotes the neutrons or protons. Shown in Fig. 5 are the relative kinetic energy distribution of nucleons with local densities higher than ρ_0 at the maximum compress stage. For clarity, we show the results of reactions $^{132}\text{Sn} + ^{124}\text{Sn}$ with a certain L . Obviously, for the energetic nucleons above a certain kinetic energy, the values of R_1^i is larger than that of R_2^i , and both of them are larger than 1, indicating that the stronger nuclear symmetry potential increases (decreases) the number of high (low) energy nucleons. Naturally, these increased high energetic nucleons are responsible for the increased π^- and π^+ through the nn and pp inelastic channels. Third, compared with the S π RIT data, our results on both π^- and π^+ yields with a certain range of $U_{sym}^\infty(\rho_0)$ can indeed fit the experimental pion data. This finding naturally provides the opportunity to constrain the value of $U_{sym}^\infty(\rho_0)$ through comparing the pion yields of theoretical simulations with the corresponding data in HICs.

Shown in Fig. 6 are the π^-/π^+ ratios of theoretical simulations for the same reactions in comparison with the S π RIT data. First, consistent with the observations of most transport models, it is seen from the upper windows of Fig. 6 that the π^-/π^+ ratios indeed are more sensitive to the L compared to the pion yields, and a softer nuclear symmetry energy with a smaller L value leads to a higher π^-/π^+ ratio, reflecting a more neutron-rich participant region formed in the reaction. Moreover, for the more neutron-rich reaction $^{132}\text{Sn} + ^{124}\text{Sn}$, the π^-/π^+ ratios show more sensitivities to the L . Second, it is seen from the lower windows of Fig. 6 that with a certain L value the π^-/π^+ ratios are indeed increasing with the value of $|U_{sym}^\infty(\rho_0)|$, reflecting a larger isospin effects resulting from the stronger nuclear symmetry potential as aforementioned. Actually, similar as that for more pion production, this observation can also be understood by examining the kinetic energy distribution of neutrons over protons with local densities higher than ρ_0 at the maximum compress stage in reactions $^{132}\text{Sn} + ^{124}\text{Sn}$ with a certain L as shown in Fig. 7. In addition, compared with the S π RIT data, our results on π^-/π^+ ratios also fit quite well the experimental data within a certain range for the value of $U_{sym}^\infty(\rho_0)$.

As a more clean observable, the double ratio of two reactions, i.e., DR(π^-/π^+) ratio of reactions $^{132}\text{Sn} + ^{124}\text{Sn}$ over $^{108}\text{Sn} + ^{112}\text{Sn}$, has the advantages of reducing both the isoscalar potential effects and the Coulomb field effects, and thus is expected to disentangle the effects of nuclear symmetry potential/energy from those of both isoscalar potentials and Coulomb fields in HICs. Therefore, we show in Fig. 8 the DR(π^-/π^+) ratios of two reactions in comparison with the S π RIT data. It is seen from

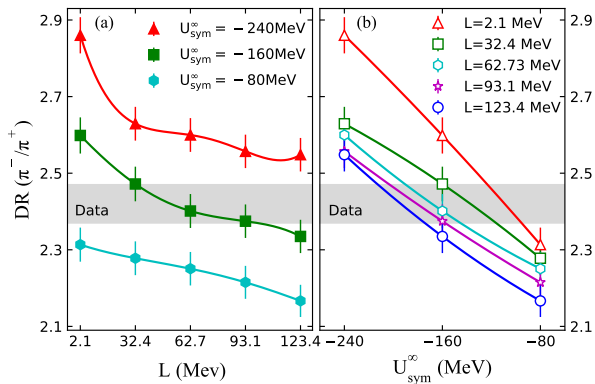


FIG. 8. (Color online) The double π^-/π^+ ratios [i.e., $DR(\pi^-/\pi^+)$] of the reactions $^{132}\text{Sn} + ^{124}\text{Sn}$ over $^{108}\text{Sn} + ^{112}\text{Sn}$ with different $U_{sym}^\infty(\rho_0)$ as a function of the L (a) and different L as a function of the $U_{sym}^\infty(\rho_0)$ (b) in comparison with the corresponding S π RIT data.

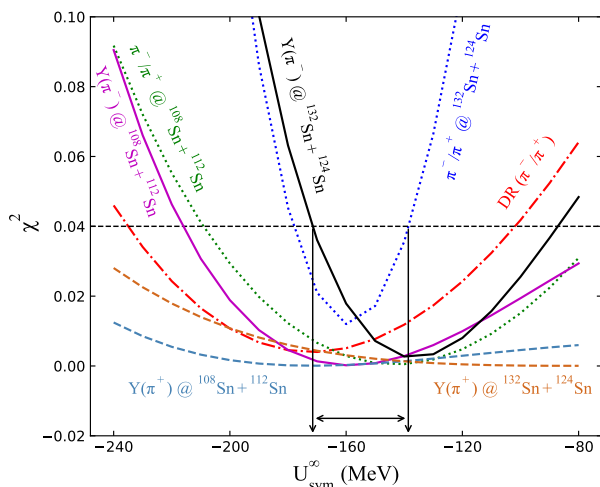


FIG. 9. (Color online) The χ -square analyses for the pion yields as well as their single and double pion ratios.

the left panel of Fig. 8 that the $DR(\pi^-/\pi^+)$ ratios of two reactions indeed are more sensitive to the high density nuclear symmetry energy. Moreover, the $DR(\pi^-/\pi^+)$ ratios are also more clearly separated by varying the value of $U_{sym}^\infty(\rho_0)$ from -80 to -240 MeV, and thus more sensitive to the momentum dependence of nuclear symmetry potential as indicated in the right panel of Fig. 8.

Now, we use above three observables, i.e., pion yields and their single π^-/π^+ as well as double $DR(\pi^-/\pi^+)$ ratios, to constrain the value of $U_{sym}^\infty(\rho_0)$. To this end, we perform the systematic χ -square analyses for pion yields as well as their single π^-/π^+ and double $DR(\pi^-/\pi^+)$ ratios at different $U_{sym}^\infty(\rho_0)$. Apart from the pion yields as well as their single π^-/π^+ and double $DR(\pi^-/\pi^+)$ ratios at $U_{sym}^\infty(\rho_0) = -80, -160$ and -240 MeV, the values of these observables at other $U_{sym}^\infty(\rho_0)$ with an interval

of 10 MeV are obtained by interpolating the simulation ones. Moreover, to extract more accurate constraints on $U_{sym}^\infty(\rho_0)$, the values of L are limited from 32.4 to 123.4 MeV since this range for L basically covers the possible range for L extracted from the existing literatures in experiments and/or theories [5, 10, 59–65]. The final χ -square analyses are shown in Fig. 9. It is seen that to ensure the errors between theoretical simulations of both pion yields and their single π^-/π^+ as well as double $DR(\pi^-/\pi^+)$ ratios and corresponding data in S π RIT experiments to be within 4% that is the maximum uncertainties of experimental data, the value of $U_{sym}^\infty(\rho_0)$ should be constrained between -171.5 and -138.6 MeV as indicated by the arrows in Fig. 9. On the other hand, it is well known that the isospin splitting of in-medium nucleon effective mass is resulting from the momentum dependence of nuclear symmetry potential. As a result, according to the formula of nucleon effective mass, i.e.,

$$m_\tau^*/m = \left[1 + \frac{m}{k_\tau} \frac{dU_\tau}{dk}\right]^{-1}, \quad (11)$$

the neutron-proton effective mass splitting Δm_{np}^* for the reaction $^{132}\text{Sn} + ^{124}\text{Sn}$ is also constrained between 0 and 0.144 MeV. Interestingly, it is noticed that the value of 0 MeV for Δm_{np}^* obtained here is consistent with that in Ref. [10].

IV. SUMMARY

In conclusion, we have studied effects of the momentum dependent characteristic parameter $U_{sym}^\infty(\rho_0)$ of nuclear symmetry potential on pion production in central Sn + Sn collisions at 270 MeV/nucleon. It is found that with a certain L value the stronger nuclear symmetry potential with the larger value of $|U_{sym}^\infty(\rho_0)|$ can lead to more production of π^- and π^+ as well as the larger pion ratios. This naturally provides the opportunity to constrain the value of $U_{sym}^\infty(\rho_0)$ through comparing the pion observable of theoretical simulations with the corresponding data in HICs. Therefore, through conducting the systematic χ -square analyses for pion observables of reactions $^{108}\text{Sn} + ^{112}\text{Sn}$ and $^{132}\text{Sn} + ^{124}\text{Sn}$, we find that the value of $U_{sym}^\infty(\rho_0)$ can be constrained at $U_{sym}^\infty(\rho_0) = -155.05 \pm 16.45$ MeV that can ensure the errors between theoretical simulations of pion observables and corresponding data in S π RIT experiments to be within 4%. Moreover, considering that the isospin splitting of in-medium nucleon effective mass is resulting from the momentum dependence of nuclear symmetry potential, we have also discussed the neutron-proton effective mass splitting.

ACKNOWLEDGMENTS

G.F.W. would like to thank Profs. B. A. Li and G. C. Yong for helpful discussions. This work is supported by

the National Natural Science Foundation of China under grant Nos.11965008, 11405128, and Guizhou Provin-

cial Science and Technology Foundation under Grant No.[2020]1Y034, and the PhD-funded project of Guizhou Normal university (Grant No.GZNUD[2018]11).

-
- [1] S. Typel, and B. A. Brown, *Phys. Rev. C* **64**, 027302 (2001).
- [2] E. E. Kolomeitsev, C. Hartnack, H. W. Barz, M. Bleicher, E. Bratkovskaya, W. Cassing, L. W. Chen, P. Danielewicz, C. Fuchs, T. Gaitanos, C. M. Ko, A. Larionov, M. Reiter, Gy. Wolf and J. Aichelin, *J. Phys. G:Nucl. Part. Phys.* **31**, S741 (2005).
- [3] V. Baran, M. Colonna, V. Greco and M. Di Toro, *Phys. Rep.* **410**, 335 (2005).
- [4] B.A. Li, L.W. Chen and C.M. Ko, *Phys. Rep.* **464**, 113 (2008).
- [5] A. Tamii, I. Poltoratska, P. von-Neumann-Cosel, Y. Fujita, T. Adachi, C. A. Bertulani, J. Carter, M. Dozono, H. Fujita, K. Fujita *et al.*, *Phys. Rev. Lett.* **107**, 062502 (2011).
- [6] X. Viñas, M. Centelles, X. Roca-Maza, and M. Warda, *Eur. Phys. J. A* **50**, 27 (2014)
- [7] C. J. Horowitz, E. F. Brown, Y. Kim, W. G. Lynch, R. Michaels, A. Ono, J. Piekarewicz, M. B. Tsang, and H. H. Wolter, *J. Phys. G:Nucl. Part. Phys.* **41**, 093001 (2014).
- [8] P. G. Reinhard, and W. Nazarewicz, *Phys. Rev. C* **93**, 051303 (2016).
- [9] M. Baldo, G. F. Burgio, *Prog. Part. Nucl. Phys.* **91**, 203 (2016).
- [10] J. Estee, W. G. Lynch, C. Y. Tsang, J. Barney, G. Jhang, M. B. Tsang, R. Wang, M. Kaneko *et al.* (S π RIT Collaboration), and M. D. Cozma, *Phys. Rev. Lett.* **126**, 162701 (2021).
- [11] C. Y. Tsang, M. B. Tsang, P. Danielewicz, F. J. Fattoyev, and W. G. Lynch, *Phys. Lett. B* **796**, 1 (2019).
- [12] Y. Lim and J. W. Holt, *Phys. Rev. Lett.* **121**, 062701 (2018).
- [13] I. Tews, J. Margueron, and S. Reddy, *Phys. Rev. C* **98**, 045804 (2018).
- [14] A. Drago, A. Lavagno, G. Pagliara, and D. Pigato, *Phys. Rev. C* **90**, 065809 (2014).
- [15] A. W. Steiner, and S. Gandolfi, *Phys. Rev. Lett.* **108**, 081102 (2012).
- [16] C. Ducoin, J. Margueron, C. Providência, and I. Vidaña, *Phys. Rev. C* **83**, 045810 (2011).
- [17] J. M. Lattimer, and M. Prakash, *Phys. Rep.* **621**, 127 (2016).
- [18] B. A. Brown, *Phys. Rev. Lett.* **111**, 232502 (2013).
- [19] P. Danielewicz, R. Lacey, and W. G. Lynch, *Science* **298**, 1592 (2002).
- [20] M. Oertel, M. Hempel, T. Klähn, and S. Typel, *Rev. Mod. Phys.* **89**, 015007 (2017).
- [21] G. W. Hoffmann, and W. R. Coker, *Phys. Rev. Lett.* **29**, 227 (1972).
- [22] A. J. Koning *et al.*, *Nucl. Phys. A* **713**, 231 (2003).
- [23] J. P. Jeukenne, C. Mahaux, and R. Sartor, *Phys. Rev. C* **43**, 2211 (1991).
- [24] G. Jhang, J. Estee, J. Barney, G. Cerizza, M. Kaneko, J. W. Lee, W. G. Lynch, T. Isobe *et al.* (S π RIT Collaboration), M. Colonna, D. Cozma, P. Danielewicz, H. Elfner, N. Ikeno, C. M. Ko, J. Mohs, D. Oliinychenko *et al.* (TMEP Collaboration), *Phys. Lett. B* **813**, 136016 (2021).
- [25] R. Shane, A. B. McIntosh, T. Isobe, W. G. Lynch, H. Baba, J. Barney, Z. Chajecki, M. Chartier, *et al.*, *Nuclear Instruments and Methods in Physics Research A* **784**, 513 (2015).
- [26] W. Reisdorf *et al.* (FOPI Collaboration), *Nucl. Phys. A* **781**, 459 (2007); *Nucl. Phys. A* **848**, 366 (2010); *Nucl. Phys. A* **876**, 1 (2012).
- [27] G. C. Yong, *Phys. Rev. C* **104**, 014613 (2021).
- [28] R. Subedi, R. Shneor, P. Monaghan, B. D. Anderson, K. Aniol, J. Annand, J. Arrington and H. Benaoum *et al.*, *Science* **320**, 1476 (2008).
- [29] L. B. Weinstein, E. Piaseutzky, D. W. Higinbotham, J. Gomez, O. Hen, and R. Shneor, *Phys. Rev. Lett.* **106**, 052301 (2011).
- [30] M. M. Sargsian, *Phys. Rev. C* **89**, 034305 (2014).
- [31] C. Ciofi degli Atti, *Phys. Rep.* **590**, 1 (2015).
- [32] O. Hen, M. Sargsian, L. B. Weinstein, E. Piaseutzky, H. Hakobyan *et al.*, *Science* **346**, 614 (2014).
- [33] M. Duer, O. Hen, E. Piaseutzky, H. Hakobyan, L. B. Weinstein, M. Braverman, E. O. Cohen, D. Higinbotham *et al.* (CLAS Collaboration), *Nature* **560**, 617 (2018).
- [34] K. A. Brueckner, J. Dabrowski, *Phys. Rev.* **134**, B722 (1964).
- [35] J. Dabrowski, P. Haensel, *Phys. Rev. C* **7**, 916 (1973).
- [36] J. Dabrowski, P. Haensel, *Can. J. Phys.* **52**, 1768 (1974).
- [37] C. B. Das, S. Das Gupta, C. Gale, and B. A. Li, *Phys. Rev. C* **67**, 034611 (2003).
- [38] B. A. Li, C. B. Das, S. Das Gupta, and C. Gale, *Phys. Rev. C* **69**, 011603(R) (2004).
- [39] L. W. Chen, B. A. Li, A note of an improved MDI interaction for transport model simulations of heavy ion collisions (Unpublished, Texas A&M University-Commerce, 2010).
- [40] C. Xu, B. A. Li, *Phys. Rev. C* **81**, 044603 (2010).
- [41] L. W. Chen, C. M. Ko, B. A. Li, C. Xu, and J. Xu, *Eur. Phys. J. A* **50**, 29 (2014).
- [42] G. F. Wei, C. Xu, W. Xie, Q. J. Zhi, S. G. Chen, and Z. W. Long, *Phys. Rev. C* **102**, 024614 (2020).
- [43] J. Dechargé, D. Gogny, *Phys. Rev. C* **21**, 1568 (1980).
- [44] J. Xu, L. W. Chen, and B. A. Li, *Phys. Rev. C* **91**, 014611 (2015).
- [45] H. Y. Kong, J. Xu, L. W. Chen, B. A. Li, and Y. G. Ma, *Phys. Rev. C* **95**, 034324 (2017).
- [46] S. Hama, B. C. Clark, E. D. Cooper, H. S. Sherif, and R. L. Mercer, *Phys. Rev. C* **41**, 2737 (1990).
- [47] O. Buss, T. Gaitanos, K. Gallmeister, H. van Hees, M. Kaskulov, O. Lalakulich, A. B. Larionov, T. Leitner, J. Weil, and U. Mosel, *Phys. Rep.* **512**, 1 (2012).
- [48] M. Ericson, T. E. O. Ericson, *Ann. of Phys.* **36**, 323 (1966).
- [49] C. García-Recio, E. Oset, and L. L. Salcedo, *Phys. Rev. C* **37**, 194 (1988).
- [50] J. Nieves, E. Oset, and C. García-Recio, *Nucl. Phys. A* **554**, 554 (1993).

- [51] G. F. Wei, C. Liu, X. W. Cao, Q. J. Zhi, W. J. Xiao, C. Y. Long, and Z. W. Long, *Phys. Rev. C* **103**, 054607 (2021).
- [52] J. Xu, L. W. Chen, C. M. Ko, B. A. Li, and Y. G. Ma, *Phys. Rev. C* **87**, 067601 (2013).
- [53] J. Hong, P. Danielewicz, *Phys. Rev. C* **90**, 024605 (2014).
- [54] T. Song, C. M. Ko, *Phys. Rev. C* **91**, 014901 (2015).
- [55] Z. Zhang, and C. M. Ko, *Phys. Rev. C* **95**, 064604 (2017).
- [56] G. F. Wei, B. A. Li, G. C. Yong, L. Ou, X. W. Cao, and X. Y. Liu, *Phys. Rev. C* **97**, 034620 (2018).
- [57] G. F. Wei, G. C. Yong, L. Ou, Q. J. Zhi, Z. W. Long, and X. H. Zhou, *Phys. Rev. C* **98**, 024618 (2018).
- [58] B. A. Li, G. C. Yong, and W. Zuo, *Phys. Rev. C* **71**, 014608 (2005).
- [59] J. M. Lattimer, and Y. Lim, *Astrophys. J.* **771**, 51 (2013).
- [60] X. Roca-Maza, X. Viñas, M. Centelles, B. K. Agrawal, G. Colò, N. Paar, J. Piekarewicz, and D. Vretenar, *Phys. Rev. C* **92**, 064304 (2015).
- [61] P. Russotto, S. Gannon, S. Kupny, P. Lasko, L. Acosta, M. Adamczyk, A. Al-Ajlan, M. Al-Garawi *et al.*, *Phys. Rev. C* **94**, 034608 (2016).
- [62] K. Hebeler, J. M. Lattimer, C. J. Pethick, and A. Schwenk, *Phys. Rev. Lett.* **105**, 161102 (2010).
- [63] I. Tews, T. Krüger, K. Hebeler, and A. Schwenk, *Phys. Rev. Lett.* **110**, 032504 (2013).
- [64] D. Lonardoni, I. Tews, S. Gandolfi, and J. Carlson, *Phys. Rev. Res.* **2**, 022033 (2020).
- [65] C. Drischler, R. J. Furnstahl, J. A. Melendez, and D. R. Phillips, *Phys. Rev. Lett.* **125**, 202702 (2020).